

# Localized Plasmon resonance in metal nanoparticles using Mie theory

J.S. Duque<sup>1</sup>, J.S. Blandón<sup>1</sup>, H. Riascos<sup>1</sup>.

<sup>1</sup>Grupo Plasma, Láser y Aplicaciones, Universidad Tecnológica de Pereira, Colombia.

E-mail: joseduque@utp.edu.co

**Abstract.** In this work, scattering light by colloidal metal nanoparticles with spherical shape was studied. Optical properties such as diffusion efficiencies of extinction and absorption  $Q_{ext}$  and  $Q_{abs}$  were calculated using Mie theory. We employed a MATLAB program to calculate the Mie efficiencies and the radial dependence of electric field intensities emitted for colloidal metal nanoparticles (MNPs). By UV-Vis spectroscopy we have determined the LSPR for Cu nanoparticles (CuNPs), Ni nanoparticles (NiNPs) and Co nanoparticles (CoNPs) grown by laser ablation technique. The peaks of resonances appear in 590nm, 384nm and 350nm for CuNPs, NiNPs and CoNPs respectively suspended in water. Changing the medium to acetone and ethanol we observed a shift of the resonance peaks, these values were agree with our simulations results.

## 1. Introduction

The optical properties of nanostructures, especially metal nanoparticles have taken great relevance due to many applications in catalysis process, plasmonics, optoelectronics, sensors and medicine. Nanoparticles are very interesting since show exotic properties such as the electric field confinement and Localized Surface Plasmons Resonances (LSPR) the latter is a phenomena characteristic of metallic nanoparticles, which is produced by charge oscillation in the surface of NP's in presence of an electric field. In spherical metal nanoparticles these are known as Fröhlich resonances (Bohren and Huffman 1983) [1, 2], and are the fundamental electric dipole resonances of spheres [3, 4]. In recent years several authors have investigated the LSPR characteristics for metal nanoparticles with spherical shape using simulations based on the Mie theory, in order to understand the behaviour of the optical properties of MNP's when changing the liquid environment or some of the parameters of growth, like show Hossein and collaborators in your work [5].

There are many techniques to obtained colloidal MPNs, including chemical and physical methods [6], in this paper MNPs were fabricated by laser ablation technique, this method of synthesis is simple and relatively fast, so that nanoparticles can be synthesized with a variety of forms and chemical natures [7]. By UV-Vis absorbance spectra we can to determine the regions where the radiation absorption has a maximum for colloidal metal nanoparticles grown by laser ablation with spherical shape. The electric filed intensities emitted for MNPs of different sizes were measured by nanoparticle tracking analysis (NTA) method, in each kind of MNPs. The electric field intensities of



MNPs too were analysed by simulation of Mie theory, also using this theory we could found the relationship of the peaks present in the scattering spectra with the LSPR for CuNPs, NiNPs and CoNPs. The dependence of the peaks shifted with the liquid environment change was determined.

## 2. Theory

Gustav Mie (1908) in his most popular work “*contributions to the optics of diffuse media, especially colloid metal solutions*” solved Maxwell’s equations for the case of an incoming wave interacting with a spherical colloidal particle [1]. For the theoretical solution he considered a plane electromagnetic wave hits a smooth spherical particle embedded in a liquid medium with a real refractive index. The particle can be metallic, thus it can be absorbing and its refractive index is, in general, a complex number. In essence, the electromagnetic fields are expanded in multipolar contributions, and the expansion coefficients are found by applying the correct boundary conditions for electromagnetic fields at the interface between the metal nanoparticles and its surrounding medium. Mie introduced spherical coordinates system, used the dimensionless size parameter  $x = 2\pi mR/\lambda_0$ , where  $R$  is the particle radius,  $m$  is the real refractive index and  $\lambda_0$  is the incident wavelength. For the solutions of electromagnetic fields Mie introduced the extinction, absorption and scattering diffusion efficiencies,  $Q_{ext}$ ,  $Q_{abs}$  and  $Q_{sca}$  known as Mie efficiencies of a spherical NP with area  $\pi R^2$ , this efficiencies are the cross section of extinction, absorption and scattering normalized per area unit and it is given by the following expressions [5, 8]:

$$Q_{ext} = \frac{\sigma_{ext}}{\pi R^2} = \frac{2}{x^2} \sum_{n=0}^{\infty} (2n+1) \Re(a_n + b_n) \quad (1)$$

$$Q_{sca} = \frac{\sigma_{sca}}{\pi R^2} = \frac{2}{x^2} \sum_{n=0}^{\infty} (2n+1) (|a_n| + |b_n|) \quad (2)$$

$$Q_{abs} = Q_{ext} - Q_{sca} \quad (3)$$

$$a_n = \frac{\psi_n(x)\psi'_n(mx) - m\psi_n(mx)\psi'_n(x)}{\xi_n(x)\psi'_n(mx) - m\psi_n(mx)\xi'_n(x)} \quad (4)$$

$$b_n = \frac{m\psi_n(x)\psi'_n(mx) - \psi_n(mx)\psi'_n(x)}{m\xi_n(x)\psi'_n(mx) - \psi_n(mx)\xi'_n(x)} \quad (5)$$

$\psi_n(x)$  and  $\xi_n(x)$  represent the Riccati-Bessel functions and it is described by the following expression.

$$\psi_n(x) = \sqrt{\frac{\pi x}{2}} J_{n+\frac{1}{2}}(x) \quad (6)$$

$$\xi_n(x) = \sqrt{\frac{\pi x}{2}} [J_{n+\frac{1}{2}}(x) + i Y_{n+\frac{1}{2}}(x)] \quad (7)$$

$J_n(x)$  y  $Y_n(x)$  are the Bessel functions of first and second kind respectively [9, 10].

Using the Rayleigh approximation, diffused electromagnetic fields can be approximated, since the first terms of the Mie coefficients are dominant [11, 12].

$$a_1^e = -\frac{i2x^3}{3} \frac{\varepsilon-1}{\varepsilon+2} + O(x^5) \quad (8)$$

$$b_1^m = -\frac{i2x^3}{3} \frac{\mu-1}{\mu+2} + O(x^5) \quad (9)$$

In equation (9),  $\mu = 1$  (for materials in the visible range), is important to note in equation (8), when  $\varepsilon = -2$ ,  $a_1^e$  becomes infinite, if  $a_1^e$  becomes infinite,  $Q_{ext}$  and  $Q_{sca}$  both become infinite also; this cannot be possible in nature. Nevertheless focusing a particular wavelength on certain metals we can obtain a situation where  $Q_{abs}$  and  $Q_{sca}$  reached a maximum in determined wavelength, in this case one speaks of Plasmon resonances localized (LSPR), since electron cloud in the metal (electronic plasma) oscillates with maximum amplitude at that wavelength [12]. Although the Mie theory do not occupy of this kinds of plasma oscillations generally the peaks present in the scattering spectra can be interpreted like these characteristic oscillations of plasma [5, 13].

### 3. Results and Discussion

#### 3.1 Simulations results

The figure 1 shows the simulations of  $Q_{abs}$ ,  $Q_{ext}$  and  $Q_{sca}$  vs incident wavelength for CuNPs suspended in water, acetone and ethanol, in these results we could observed a particular pattern of peaks corresponding with the oscillation modes of colloidal CuNPs based on the Mie theory. In the simulation we can see the maximum of Mie efficiencies located in the region corresponding to the maximum absorption of radiation for CuNPs. Also, in the simulations we can see a dependence of nanoparticle size and the surrounding medium with peaks positions in the spectra, to change these parameters in the simulations we could observe a shift of the peaks for greater wavelength and widening of the absorption peaks, similarly it happened with NiNPs and CoNPs in the same surrounding media. These simulations were done based on the previous code developed by Mätzler for calculated the Mie scattering [11]. The simulation was done using the values suggested by (Johnson and Christy 1974) [17], for complex refractive index of material and refraction index for medium.

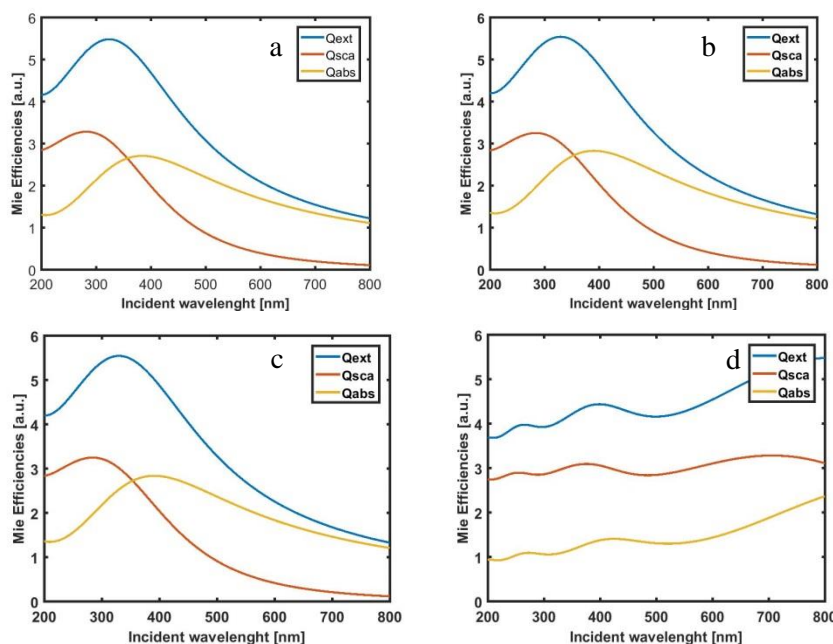


Figure 1: Simulation of Mie efficiencies  $Q_{abs}$ ,  $Q_{ext}$  and  $Q_{sca}$  for CuNPs of 40 nm, in different liquid environments a) water  $n=1,3333$ , b) acetone  $n=1,3592$  and c) ethanol  $n=1,3612$ . In subfigure d) is shown Mie efficiencies for CuNPs in water with 100nm of size.

Figure 2 shows electric field intensities vs size parameter, generated by CuNPs suspended in water, the simulations show the radial dependence of electric field intensities emitted for colloidal nanoparticles produced by the surface electron cloud interacting with light. We can see in simulations that electric field presented growth approximately in exponential form with NP's size parameter, and its maximum value is closed to the sphere surface as shown in figure 2, this maximum intensity is due to charge oscillation by the electric field confinement at the sphere surface, due to this increase in the electric field intensities near to surface is that the modes of oscillation in MNPs are generated.

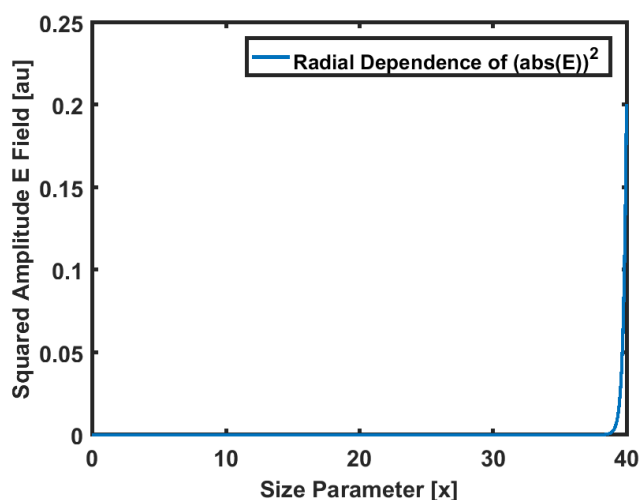


Figure 2: Simulations of radial dependence of electric field intensities in CuNPs suspended in water.

### 3.2 Experimental details

The laser ablation system to prepared MNPs in this work operates with following parameters: The pressure and temperature remained constants to room temperature. The Nd: YAG laser system (Spectra Physics Indy-10) operated at its fundamental frequency 1064 nm (first harmonic) in Q-Switch mode with rate of 20 Hz, 7 ns of pulse duration and the laser energy to growth was 300mJ. All samples were irradiating during 30 minutes. For the characterization, Evolution 201/220 UV-Visible spectrophotometer from the Thermo Scienti series of quartz cuvettes with 1 cm of optical path was used. Nano-Tracking-Analysis (NTA) was made with the NanoSight NS300 system.

### 3.3 Experimental results

Figure 3 shows the UV-Vis absorbance spectroscopy produced for CuNPs, NiNPs and CoNPs suspended in deionized water, fabricated by laser ablation method [7]. We observed the principal peaks around 250 nm for CuNPs, 230 nm for NiNPs with most intensity of absorbance due to the ferromagnetic character of Ni. For CoNPs the maximum of absorbance is in 200 nm, and the intensity of absorbance between 400 nm and 700 nm is proximally to zero, it indicated that CoNPs are transparent for the visible radiation. The characteristics peaks of LSPR appear in 590nm, 384 and 350nm like a slight shoulder in the spectrum for CuNPs, NiNPs and CoNPs respectively suspended in water, these results are agreeing with previous results and corresponding with the LSPR band for this kind of MNPs [12, 13]. These results are in agreement with those reported by the literature, which can be corroborated by the similarity of results obtained by H.S Desarkar and collaborators [18], and those obtained in this work. Although the study by Desarkar focuses on the effect of laser radiation time on the sample and its change in absorption spectra, it is important to make this comparison since the same manufacturing method is used and some of the growth parameters are similar.

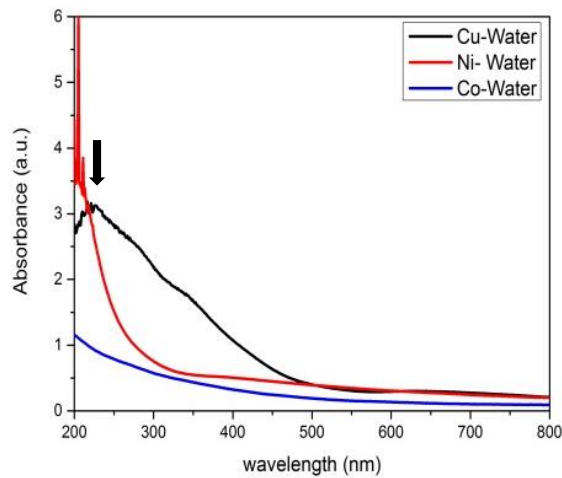


Figure 3: UV-Vis absorbance of colloidal CuNPs, NiNPs and CoNPs suspended in water grown by laser ablation technique.

In figure 4 we could observe the UV-Vis absorbance for CuNPs, NiNPs and CoNPs changing the liquid environment for acetone and we can observe a shifted of the principal peaks, for CuNPs the principal peaks appear in 340 nm and this has widening, which indicates that the CuNPs in acetone are larger than in water, it is important to note that the laser ablation method produces polydisperse NPs solutions. Moreover, that light radiation have a strongly interactions with acetone from 200nm to 300nm region, this is manifested as noise in the acetone NPs spectra. The shift of the maximum to longer wavelengths is a phenomenon of great interest because recently has been used for the design of more efficient solar cells [5]. Also the NPs based on this kind of metals are ferromagnetic at room temperature (ferromagnetic-fluid) and exhibit strong response to the interaction with radiation which as proposed for Chen and collaborators, this phenomenon has been applied to the development of Plasmonics Nano-antennas [15].

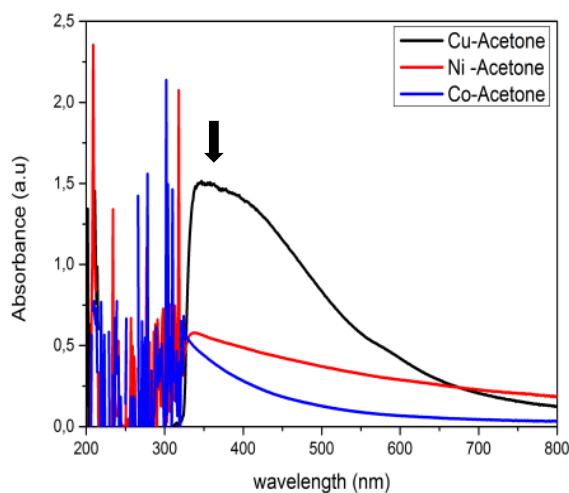


Figure 4: UV-Vis absorbance of colloidal CuNPs, NiNPs and CoNPs suspended in acetone grown by laser ablation technique.

Changing the surrounding media we observed the LSPR most defined for CuNPs suspended in ethanol located at 598nm clearly we can see resonance and we can corroborate a shift of this maximum as seen in the simulation results of the theoretical model and the UV-Vis spectra in figure 5. The peaks shifting were evidenced in the color change of the colloidal dispersions, for example colloidal CuNPs show a green color suspended in water, and colloidal CuNPs suspended in acetone show brown color, another important feature is that CuNPs in water show precipitated and agglomerated with the passage of the hours while CuNPs in acetone did not change their color and did not agglomerate.

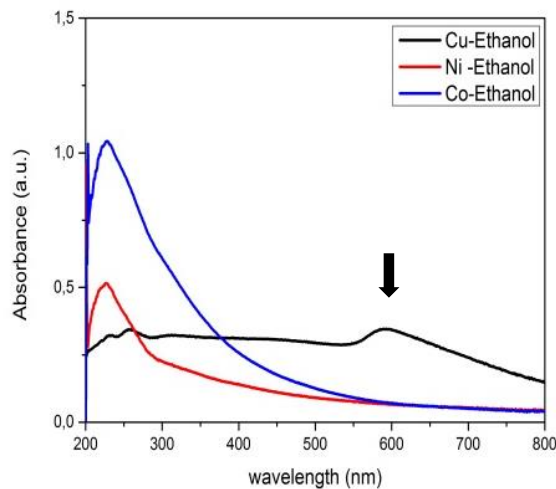


Figure 5: UV-Vis absorbance of colloidal CuNPs, NiNPs and CoNPs suspended in ethanol grown by laser ablation technique.

With this result we can observe that LSPR not only depend on the size and shape of the nanoparticles. If not also the polarization of the medium, for a higher index of refraction the dielectric function increases and therefore there will be greater polarization of the medium attenuating the accumulated charge in the resonance zone. By attenuating the electric charge of the NPs this reduces the restoring electric force, and reducing the restoring force immediately reduces the resonance frequency, that is why the absorption peaks present red-shifted.

Figure 6 shows Nano Tracking Analyzed (NTA) results in this results we can see the light scattering produced by CuNPs, NiNPs and CoNPs. In addition in figure 6a, we can see the nanoparticle-light interaction shown the characteristic scattering pattern of CuNPs, we can see the increased intensity of electric field near the edge of the nanoparticle and its strong interaction with other nanoparticles forming a characteristic dipole scattering pattern. We could found that CuNPs and NiNPs show greater absorption of radiation it is evident in NTA results show in figure 6b exhibit the intensity of CuNPs suspended in water and his relation with size of the particles, it is according with our simulations results showed in the figure 2.

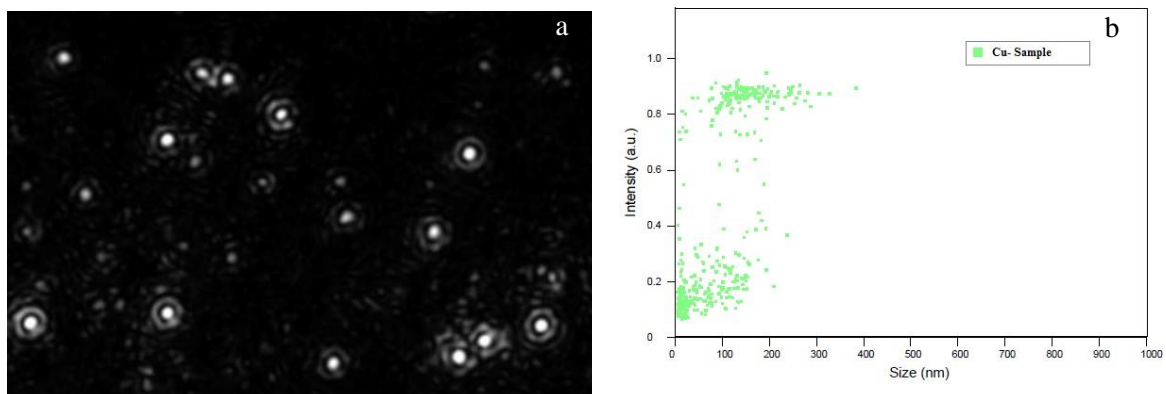


Figure 6: a) Scattering electric field pattern of MNP's using NTA method. b) Distribution of electric field intensities produced by CuNPs of different size suspended in water, grown by laser ablation technique.

#### 4. Conclusions

In summary, a theoretical model to describe the light scattering by MNPs using Mie theory were studied and simulated, also we could find the LSPR in CuNPs, NiNPs and CoNPs and determine its dependence with the size and surrounding medium, these resonances were due to charge oscillation close to the sphere surface and there show the maximum intensity of electric field, also we can see the electric field grow approximately in exponential form with NP's radius just concentrate on the surface of the sphere. We observed the principal peaks at 250 nm, 230nm and 200nm for CuNPs, NiNPs and CoNPs respectively corresponding with interband transitions. The Localized plasmon resonances appear in 590nm, 384 and 350nm for CuNPs, NiNPs and CoNPs suspended in water. LSPR most defined was for CuNPs in ethanol, and in 598nm clearly we could see these resonances by UV-Vis spectroscopy, also we could determine that the colloid of CuNPs in acetone were the most stable solution.

#### Acknowledgments

This work was supported by a grant from the *Convocatoria 738 jóvenes investigadores alianza COLCIENCIAS-SENA 2015* (Colombia).

#### References

- [1] Gustav Mie. 1908. Ann. Physics, 25(4):377-445.
- [2] Bohren, C. and D. Huffman, 1983. John Wiley and Sons, New York.
- [3] Xiaofeng Fan, Weitao Zheng, and David J Singh. 2014. Light: Science and Applications, 3(79): 1-14,
- [4] Daniel A. Cruz and Miriam C. Rodríguez and Juan M. López, (2012). Avances en Ciencias e Ingeniería 2-3, 67-78.
- [5] Hossein Ghaforyan, Majid E., and Sara Mohammadi. 2015. TI Journals World Appl. Programming, 5(4):79-82.
- [6] Charles Pool and Frank Owens. Introduction to nanotechnology. 2003. John Wiley and Sons, Inc. 107-110.
- [7] J.S. Duque, H. Riascos, G. Osorio and J.P. Cuenca 2015. El hombre y la máquina. E 47. 37-42.
- [8] Guillaume Baffou. 2012. Mie theory for metal nanoparticles. CNRS 1-2.
- [9] John David Jackson. 1999. John Wiley and Sons, Inc. Third Edition.
- [10] Kou-Nan Liu. 1977. University Utah. University Utah.
- [11] Christian Mätzler. 2002. Research Report No. 200208, Institut für Angewandte Physik.
- [12] Daniel Mazón Solórzano. 2012. Proyecto fin de Carrera Universidad de Cantabria.
- [13] V.A.G. Rivera, F.A. Ferri and E. Marega Jr. (2012). Plasmonics - Principles and Applications, Dr. Ki Young Kim (Ed.), InTech, DOI: 10.5772/50753.
- [14] M. Muniz-Miranda · C. Gellini · A. Simonelli · M. Tiberi · F. Giammanco · E. Giorgetti, 2013. Appl Phys A 110:829–833 DOI 10.1007/s00339-012-7160-7.
- [15] Jianing Chen , Pablo Albella , Zhaleh Pirzadeh , Pablo Alonso-González , Florian Huth, Stefano Bonetti (2011). Small 2011, 7, No. 16, 2341–2347. DOI: 10.1002/sml.201100640.
- [16] Helmuth Horvath. 2009. Journal of Quantitative Spectroscopy & Radiative Transfer (110) 787–799.
- [17] P. B. Johnson and R. W. Christy. 1972. Phys. Rev. B 6, 4370.
- [18] H. S. Desarkar P. Kumbhakar A. K. Mitra. 2012. Appl Nanosci 2:285291, pags. 285-291.